JOURNAL OF MATERIALS SCIENCE 25 (1990) 1537–1544

Sol–gel synthesis of zirconia barrier coatings

M. SHANE*, M. L. MECARTNEY‡
Department of Chemical Engineering and Materials Science, University of Minnesota, 421 Washington Avenue SE, Minneapolis, Minnesota 55455, USA

A method for applying zirconia barrier coatings using a sol–gel method is described. The coatings of 8 wt% yttria-stabilized zirconia are applied by spin coating a solution containing zirconium alkoxides and yttrium acetate on to stainless steel substrates. Crystallization of the films was observed for thermal treatments in the range 750 to 1050° C. Excellent adhesion at the interface, due to significant coating–substrate interfacial reactions, indicates that this sol–gel route is a feasible method for applying zirconia coatings.

1. Introduction

The use of thermal barriers in heat engines is becoming an increasingly attractive idea. By using a thermal barrier, critical engine components such as superalloy turbine airfoils can be insulated by a coating of ceramic from the high-temperature corrosive environment found in heat engines. This could lead to several important improvements in performance, including a higher engine efficiency by using higher engine temperatures, and a slower rate of corrosion from contaminants found in fuels.

Ceramic thermal barrier coatings are not a new idea. Plasma-sprayed coatings, which have a fairly high level of porosity, have been used for over a decade to reduce metal temperatures in aircraft burners and afterburners [1]. For turbine airfoil applications, however, fuel contaminants such as sodium sulphate can deposit in these pores and cause hot corrosion at the metal–ceramic interface. Because of these stringent environmental requirements, turbine airfoils with ceramic coatings have not been highly successful.

This study was undertaken to determine the feasibility of sol–gel ceramic coatings as an alternative to plasma-sprayed coatings. The requirements for thermal barrier coatings and the process of sol–gel coating are briefly reviewed before the experimental results are presented.

1.1. Thermal barrier coatings

Materials which make up barrier coatings must satisfy several criteria. Firstly, the thermal expansion of the coating must match the thermal expansion of the substrate. Secondly, the material must have a low thermal conductivity to enhance its insulating properties. Thirdly, the coating must have good thermal shock characteristics. One promising material is yttria-stabilized zirconia. In particular, compositions in the range 6 to 9 wt% yttria have been shown to have very good coating properties [1]. Zirconia has a large thermal expansion coefficient of $10 \times 10^{-6}\,°C^{-1}$. This large value matches many metals, which often are in the range 12 to $20 \times 10^{-6}\,°C$. The match is not perfect however, because there is a large variation of the thermal expansion of zirconia with temperature, and most metals do not have such a large variation.

Many ceramic materials with a large thermal expansion coefficient have poor thermal shock characteristics. However, when zirconia is only partially stabilized it can undergo a phenomena known as transformation toughening [2] which gives partially stabilized zirconia a very high fracture toughness, and enhances its resistance to thermal shock failure.

The thermal conductivity of zirconia is also very low, $0.05\,cal\,°C^{-1}\,sec^{-1}$, compared with $0.5\,cal\,°C^{-1}\,cm^{-1}\,sec^{-1}$, for many metals. This order of magnitude difference in thermal conductivities allows thin ceramic layers to act as effective thermal barriers.

1.2. Sol–gel ceramic processing

Sol–gel ceramic processing refers to a wet chemical method of producing ceramic materials [3]. The sol can be a solution of soluble organometallic precursors. The gel is a macroscopically rigid network built through polymerization.

A zirconium alkoxide, zirconium tetrabutoxide [$Zr(OCH_2CH_2CH_2CH_3)_4$], was used in this study as the zirconium source. Alkoxides undergo hydrolysis in the presence of water, usually with an acid or base catalyst, followed by condensation to give the Zr–O–Zr polymer. This polymer forms the gel which, after pyrolysis of any remaining organic groups, will form the ZrO_2 ceramic. These reactions are schematically illustrated in Fig. 1.

One problem with zirconium alkoxides is that the hydrolysis is much faster than condensation. The zirconium atoms become fully hydrolysed and form zirconium hydroxide precipitates. This is one method of forming zirconium oxide powders, but it prevents the formation of good coatings [4].

The solution to this problem is the use of acetylacetone, $CH_3COCH_2COCH_3$. This molecule forms a

Present address: Materials Science Department, University of Pittsburgh, Pennsylvania, USA.
‡Author to whom all correspondence should be addressed.

0022–2461/90 $03.00 + .12

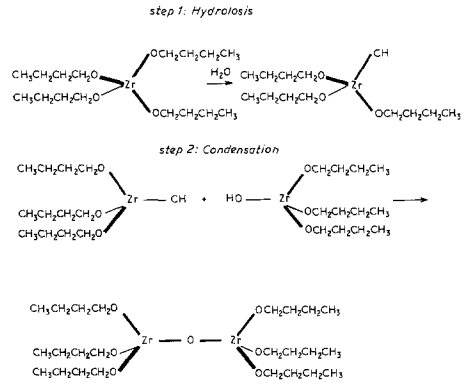

Figure 1 Reactions illustrating the sol to gel transition. The butoxy groups still attached to the zirconium atoms after the condensation are free to undergo hydrolysis, followed by further condensation to build polymer chains. After step 1, a butanol molecule is also given off together with a water molecule from step 2.

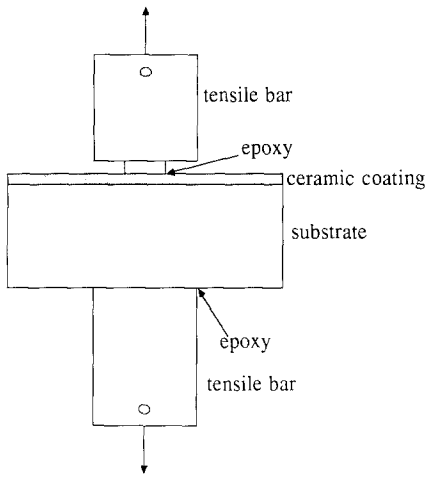

Figure 2 Tensile test for coating adhesion.

strong complex with zirconium atoms which greatly slows hydrolysis, apparently via a steric hindrance mechanism [5].

The yttrium source in this study was an aqueous solution of yttrium acetate, $[Y(O_2CCH_3)_3]$. This species does not undergo hydrolysis or condensation, and so does not become part of the gel network. However, it does become intimately mixed with the zirconium alkoxide in solution and becomes trapped in the gel structure when the solution gels.

2. Experimental procedure

This study was conducted to illustrate the feasibility of zirconia sol–gel coatings. It was decided to prepare the sol and spin coat it on a polished stainless steel substrate. Solvent evaporation during the spinning operation causes the sol to gel transition. The coatings were then heat treated and analysed.

2.1. Substrate preparation

The substrates for this study were 1.5 mm diameter discs of 446 stainless steel. The discs were machined from a bar of 446 steel, and then subjected to surface grinding with a diamond grinding wheel, lapping with 20 μm lapping slurry, and final polishing with 0.3 μm polishing compound. This left a flat, nearly mirror-like surface to be coated.

446 stainless steel was chosen for its very low thermal expansion coefficient of 12×10^{-6} °C, compared with values of 18×10^{-6} °C for austenitic steels. It does not, however, have the same variation in thermal expansion with temperature as zirconia. This stainless steel varies from 10×10^{-6} °C at room temperature to 14×10^{-6} °C near 1000° C while zirconia varies from 7.5×10^{-6} °C at 25° C to 13×10^{-6} °C near 1000° C.

2.2. Chemical preparation

Solutions to form 8 wt % yttria-stabilized zirconia were made using zirconium tetrabutoxide and yttrium acetate. Acetylacetone was added in a 1 : 1 molar ratio with the zirconium tetrabutoxide.

The mixing of the solutions was done in two parts. The first solution consisted of 16.8 g zirconium tetrabutoxide, 3.5 g acetylacetone, 15 g isopropyl alcohol as a solvent, and 1 ml concentrated nitric acid. This solution was stirred for 5 min to allow establishment of equilibrium between the zirconium tetrabutoxide and acetylacetone. Then an yttrium acetate solution composed of 11.15 g yttrium acetate, 25 g isopropyl alcohol, and 2 ml concentrated nitric acid was separately mixed then added to the first solution. Some white precipitates formed immediately upon mixture of the two solutions, but they rapidly re-dissolved. The solution was stirred for approximately 30 min, and was stable for several weeks.

2.3. Spin coating

Details of the spin-coating process can be found elsewhere [6]. The spin-coating parameters used in this study were a 2000 r.p.m. spinning rate for 60 sec. A small syringe was used to apply about 2 ml sol to each substrate before spinning was started. Once the spinning cycle was completed, the coating was almost completely dry and was ready for thermal treatment.

2.4. Thermal treatment

Based on evidence for high-density sintering of sol-based zirconia powders at 1000° C, four temperatures of 750, 850, 950 and 1050° C were selected for the thermal treatments [4].

The samples were heated from room temperature to 450° C in 20 min, and held for 15 min. The decomposition temperature of zirconium organometallic compounds is approximately 450° C [7]. The samples were subsequently brought to the maximum temperature in approximately 30 min, and then held at this temperature for 30 min. The cooling rate was fairly rapid, with the temperature reduced to room temperature in 20 to 30 min.

2.5. Characterization

Optical microscopy, scanning electron microscopy (SEM) and X-ray diffraction were used to characterize the film microstructure and phase composition. A tensile test was used to measure the coating adhesion [8]. Each of the four samples was tested by attaching a small tensile bar (diameter 0.22 mm) to the ceramic coating with epoxy and a larger tensile bar to the bottom of the substrate. The sample was then loaded in tension and the load was monitored as the tensile

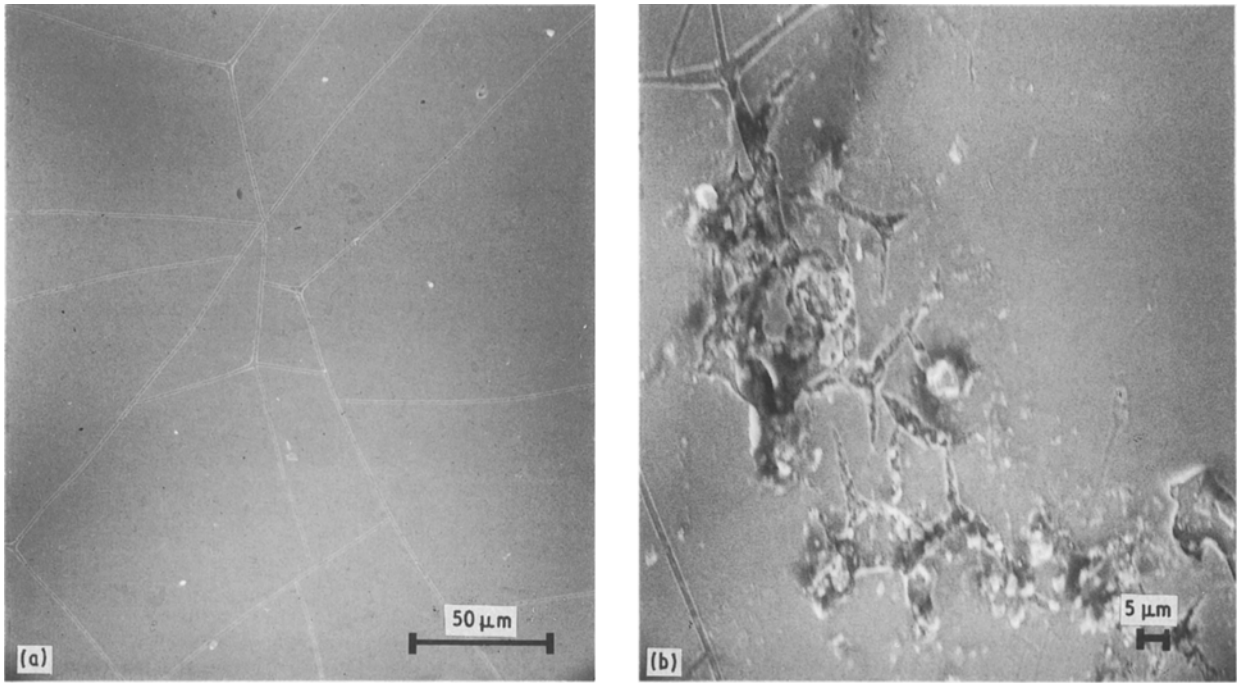

Figure 3 Scanning electron micrographs of Y_2O_3–ZrO_2 coating heat treated at 750° C. (a) Low magnification showing cracking, (b) high magnification of region with spalling.

bar pulled on the coating. The adhesive strength (S_a) was defined as S_a = maximum load/coating area fractured. Fig. 2 shows a schematic illustration of the test. The strain rate used for the test was 0.12 mm mm^{-1}.

An acid test was also conducted. The acid test consisted of placing drops of concentrated hydrochloric acid on a coated sample and an uncoated substrate. The acid was allowed to react with the material for 30 min, after which it was washed off. The surfaces of the samples were then compared for damage.

3. Results

3.1. Optical microscopy

The optical microscopy results showed strong differences in colour for the samples heat treated at different temperatures. The sample which had the 750° C thermal treatment had a fairly bright yellow colour, much the same colour as the zirconium tetrabutoxide solution. The sample at 850° C had some remnant yellow colour, but was largely a deep blue colour with some red patches scattered throughout the sample. The sample at 950° C was a brown–grey colour, with some small patches of red and blue, while the sample at 1050° C was a darker brown–grey colour.

3.2. Scanning electron microscopy

The scanning electron microscopy (SEM) results are shown in Figs 3 to 6. The surface of the 750° C sample in Fig. 3 is fairly smooth and flat, and there are cracks running through the surface, most likely due to drying stresses.

In the higher temperature sample from 850° C (Fig. 4) several cracks are still evident, although they tend to blend in with the surrounding structure much better. The surface roughness is much more evident here, and it appears that some grain structure is beginning to form.

By 950° C, the surface roughness is now the dominant feature (Fig. 5). A definite "worm-like" grain morphology is covering nearly the entire surface of the sample. Some cracks are still evident, but they are much less noticeable than earlier samples. Fig. 5b shows the grain morphology in much more detail and traces of residual cracks.

The sample heat treated at the highest temperature, 1050° C, was almost completely covered by a grainy phase (Fig. 6). There were no cracks or pores visible in this sample. The higher magnification micrograph (Fig. 6b) shows the extreme texturing and crystallization.

The coating thickness appeared to be of the order of a few micrometres after viewing a cross-section in the SEM.

3.3. X-ray diffraction

The X-ray diffraction (XRD) data are shown in Fig. 7. The peak at 45° is typical of austenitic stainless steels and appears because the coatings are thin enough for the substrate also to diffract.

Fig. 7a shows the X-ray diffraction data from the sample at 750° C. Peaks at 30°, 35.2° and 50.5° correspond to the cubic or tetragonal phases of zirconia. (More precise work at higher values of 2θ would be necessary to distinguish these two phases, but cubic and tetragonal zirconia would be the equilibrium phases with 8 wt % yttria.) The peaks are fairly weak and broad, corresponding to small amounts of very tiny crystalline particles. No other phases were found.

The X-ray data from the sample at 850° C are given in Fig. 7b. (It should be noted that the scanning rate on this sample was twice that of the other samples,

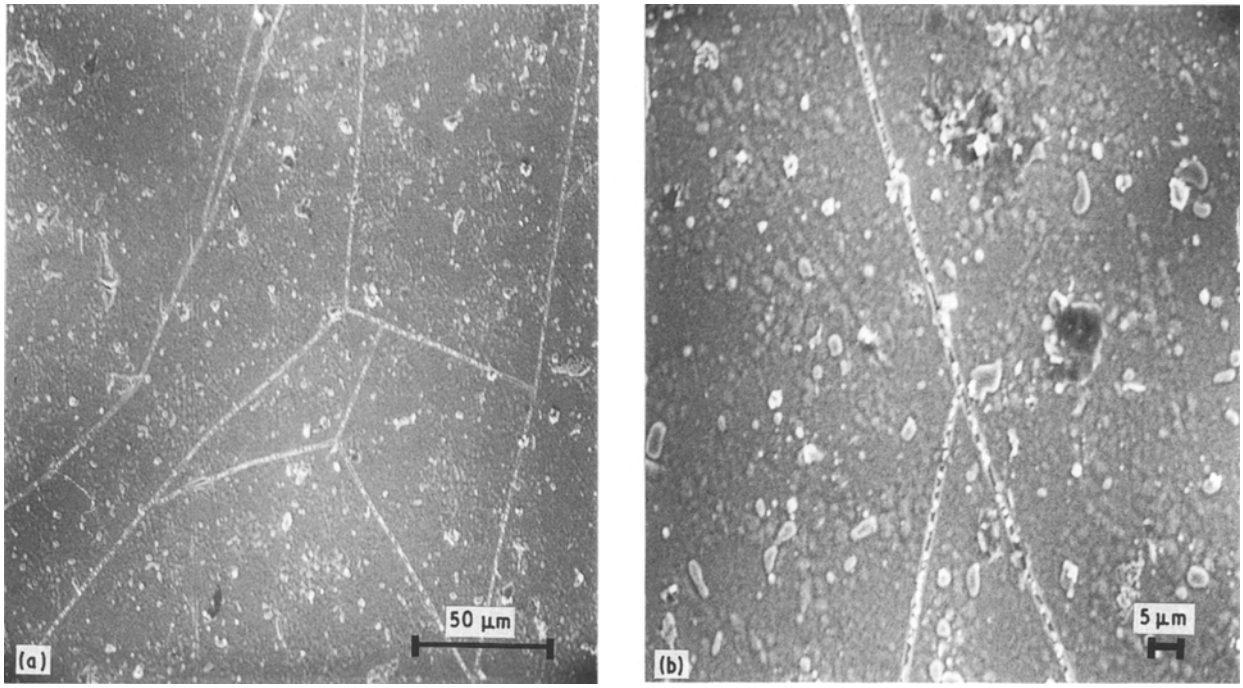

Figure 4 Scanning electron micrographs of Y_2O_3–ZrO_2 coating heat treated at 850° C. (a) Low magnification indicating some texturing; (b) high magnification showing surface cracks.

making direct peak height comparisons invalid.) Zirconia peaks once again show up at 30°, 35.2° and 50.5° 2θ, along with the substrate peaks. There is also, however, a small peak at 33.5° 2θ which corresponds to $(Fe_{0.5}Cr_{0.4})_2O_3$.

The X-ray data from the sample at 950° C are shown in Fig. 7c. The zirconia peaks are once again present, and are much stronger and sharper than in the lower temperature sample. However, there are several extra peaks present at 33.5° ($(Fe_{0.6}Cr_{0.4})_2O_3$), 36.2° and 42.6° 2θ ($FeCr_2O_4$).

Fig. 7d presents the X-ray data from the sample at 1050° C. The tetragonal cubic zirconia peaks are present, along with the substrate peaks and seven strong additional peaks due to the iron chromates.

3.4. Adhesion

The adhesion and fracture results are summarized in Table I.

3.5. Acid protection

Samples were observed for signs of corrosion, e.g. hydrogen gas evolution when subjected to concentrated hydrochloric acid for a period of 30 min. After this time the acid was washed off and the surfaces of both samples were inspected for surface damage.

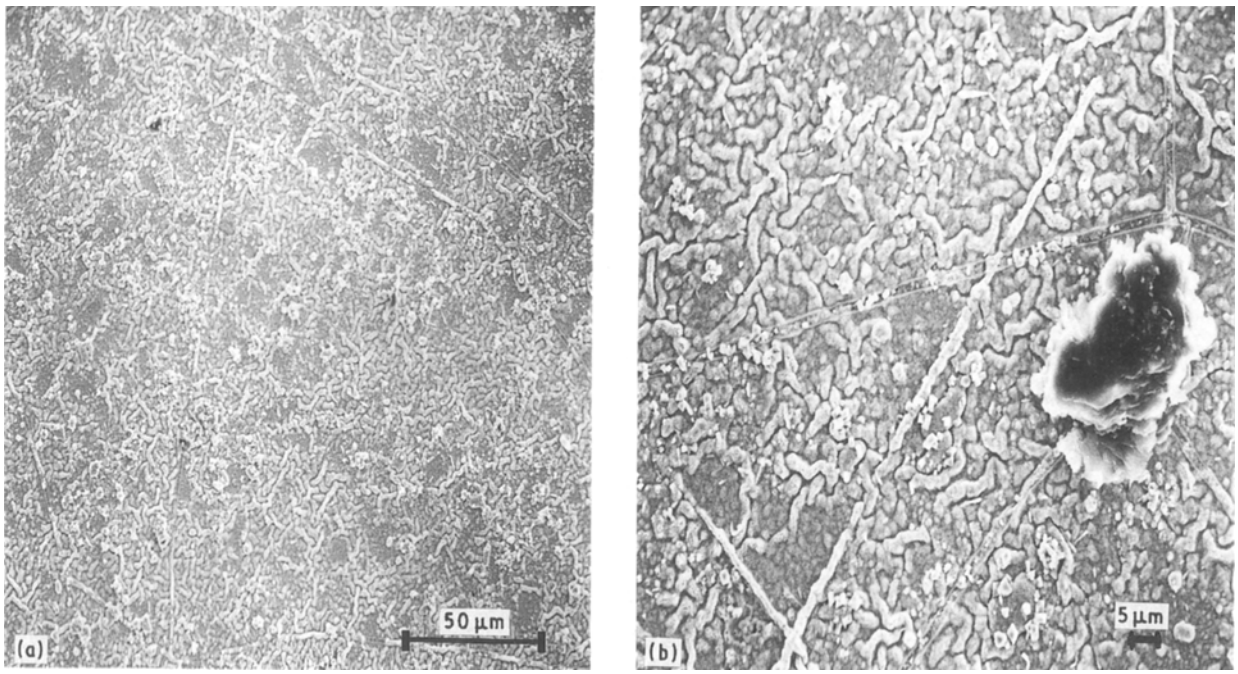

Figure 5 Scanning electron micrographs of Y_2O_3–ZrO_2 coating heat treated at 950° C. (a) Low magnification; (b) high magnification showing traces of residual cracks.

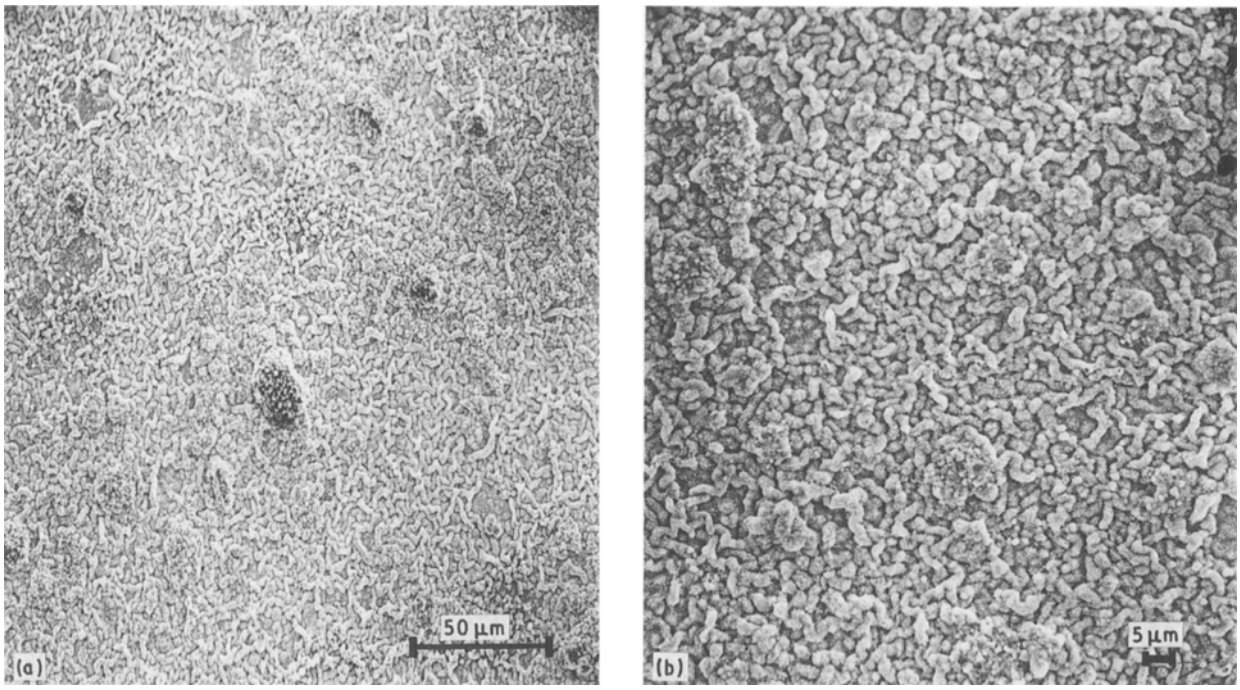

Figure 6 Scanning electron micrographs of Y_2O_3–ZrO_2 coatings heat treated at 1050° C. (a) Low magnification, (b) high magnification of the crystallized surface.

Little or no hydrogen was given off by the coated sample (1050° C), while the bare substrate bubbled furiously. The uncoated sample was badly scored, while the coated sample showed no visible signs of damage.

4. Discussion

These results show that crystallization of the ceramic coating has already begun at 750° C. The weak, broad X-ray peaks indicate the onset of crystallization at this temperature. The grains grow larger and more

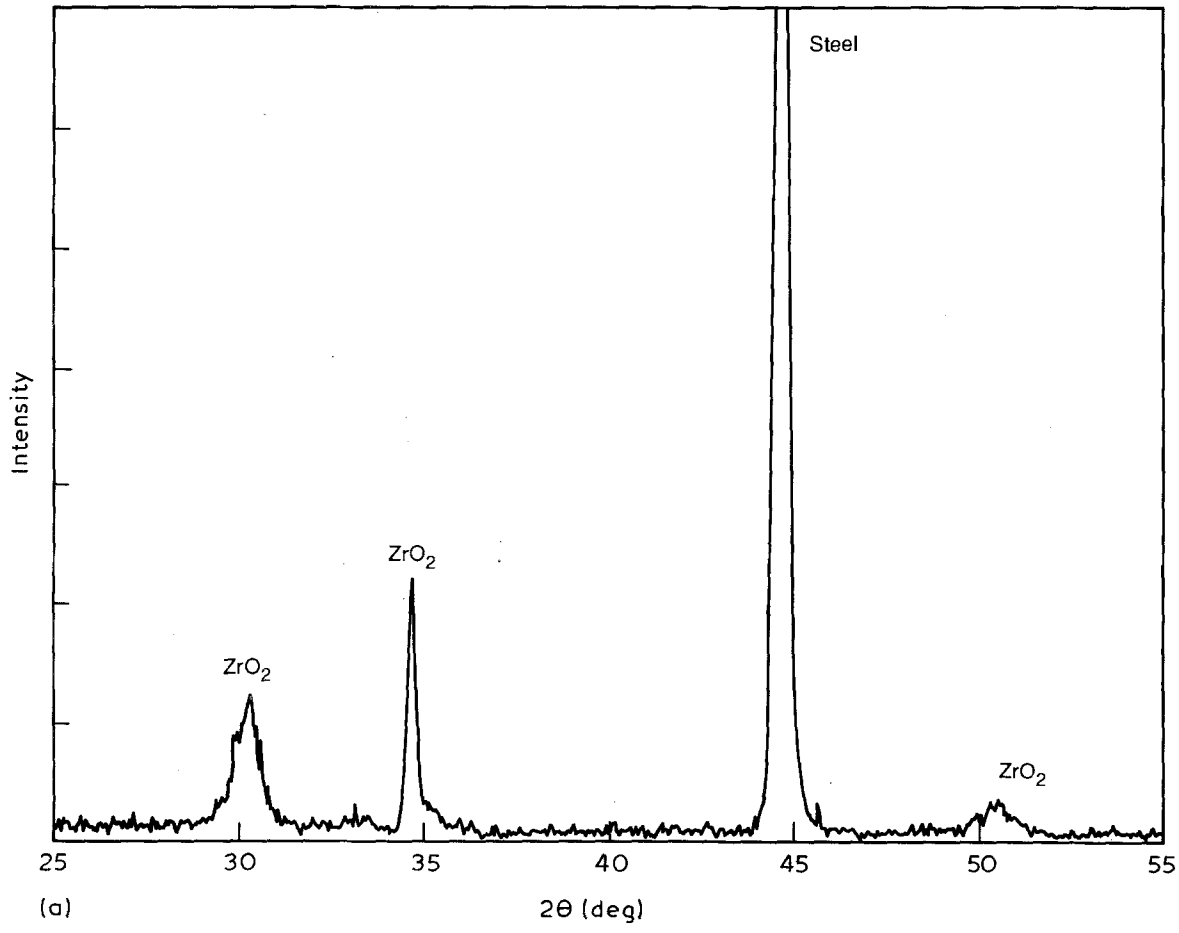

Figure 7 X-ray diffraction patterns from Y_2O_3–ZrO_2 coatings heat treated (a) at 750° C, (b) at 850° C, (c) at 950° C, and (d) at 1050° C.

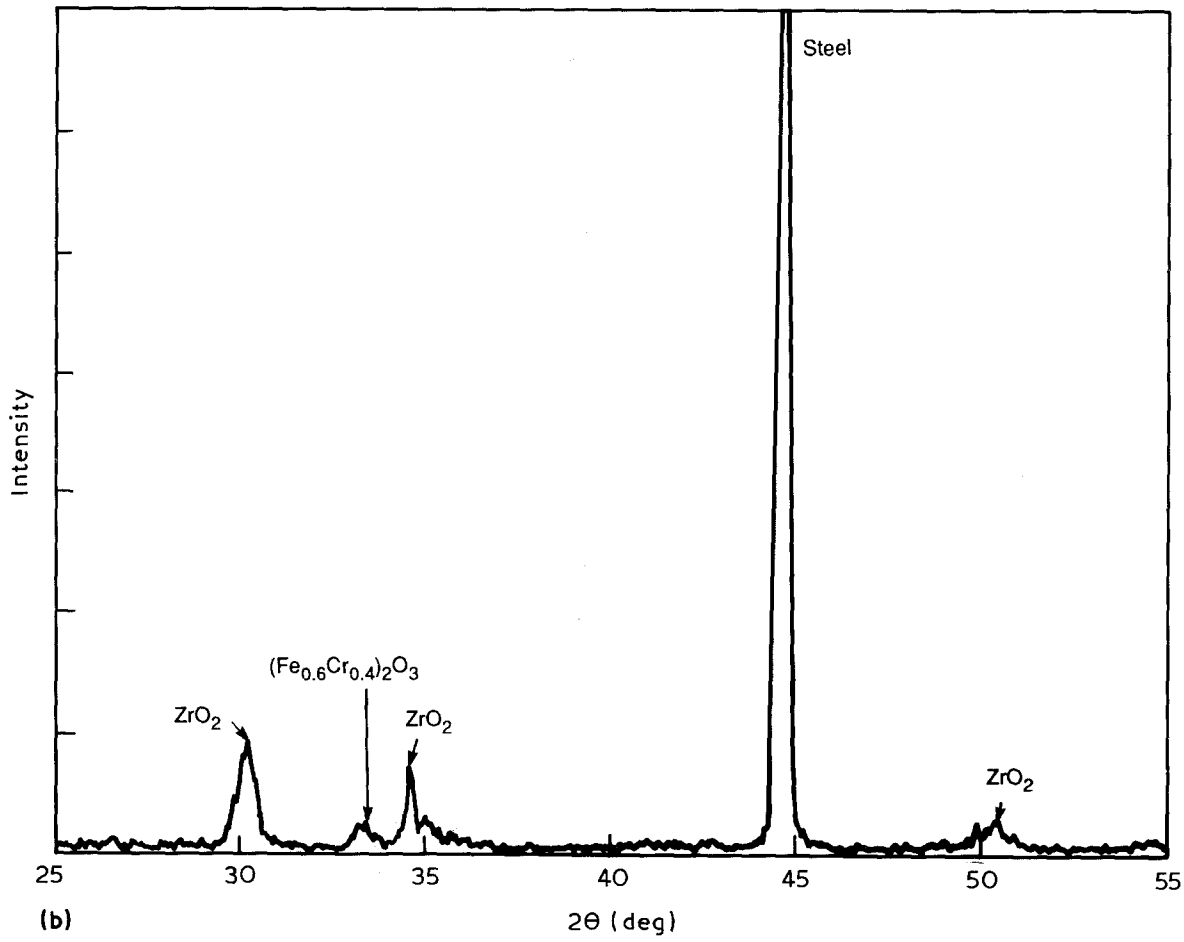

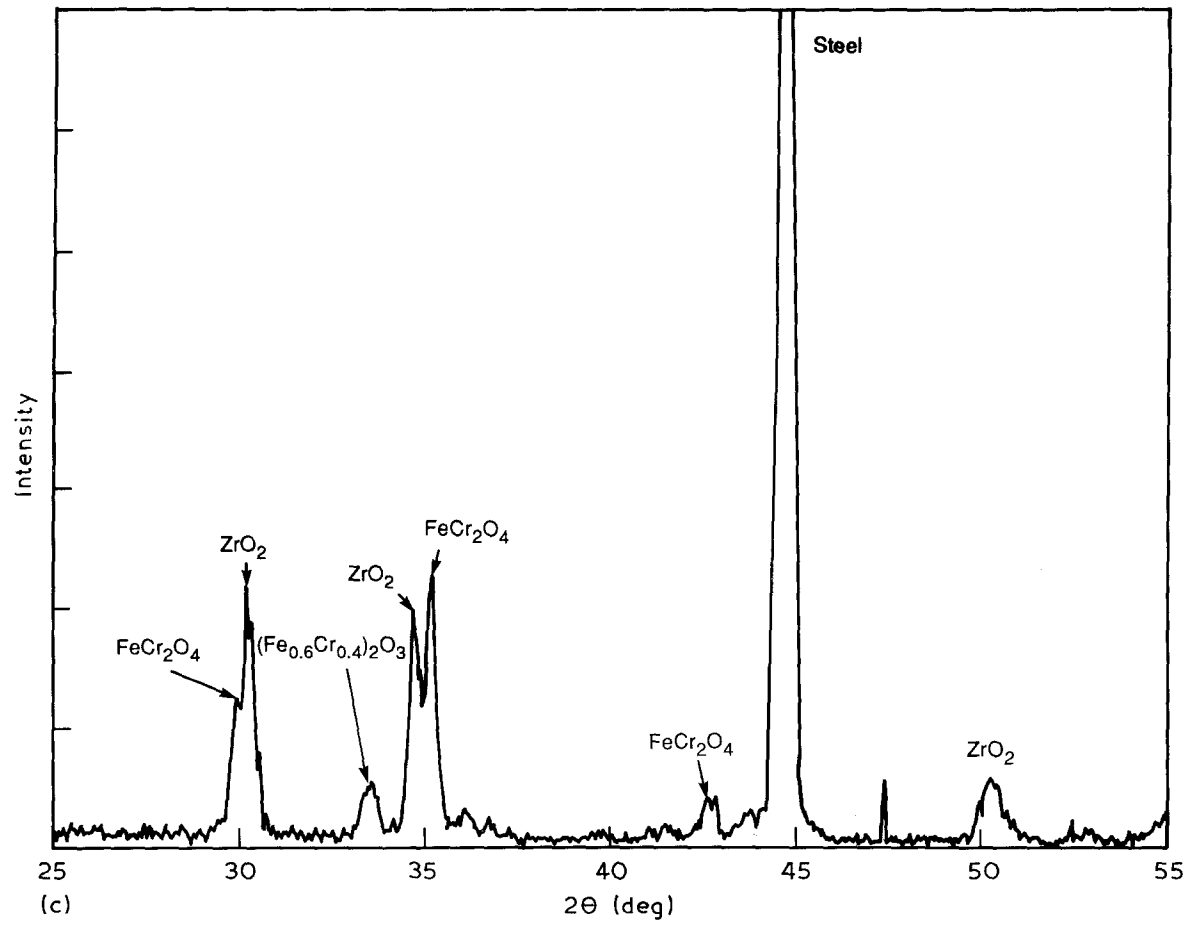

Figure 7 continued.

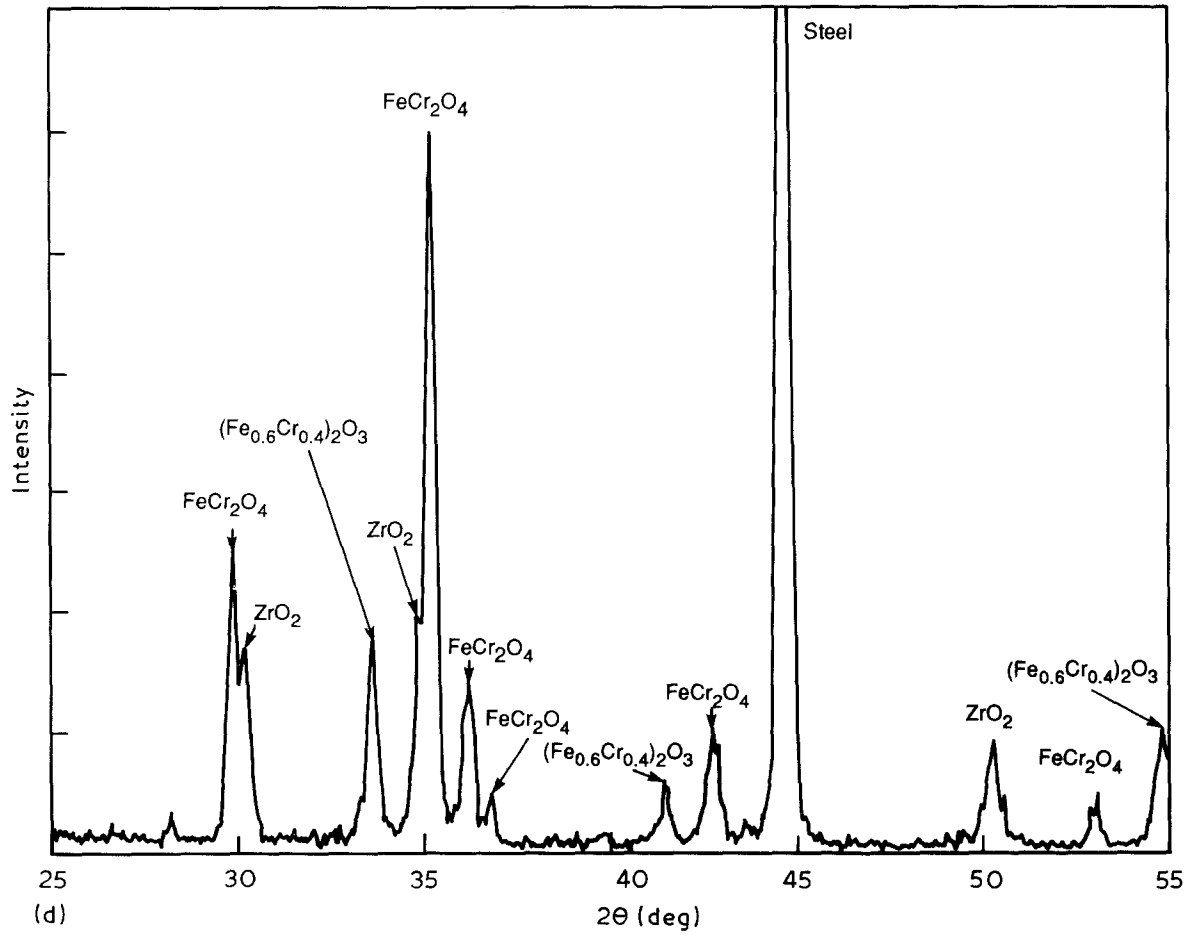

Figure 7 Continued.

pronounced, and the volume fraction of the crystalline zirconia increases as the maximum temperature encountered in the thermal treatment increases.

Coating cracks and pores are diminished in size by exposure to high temperatures. It appears that grains begin to form at 850° C. At 1050° C the cracks are indistinguishable, most likely due to grain growth healing the cracks.

The extra peaks in the X-ray diffraction data from $FeCr_2O_4$ and $(Fe_{0.6}Cr_{0.4})_2O_3$ must be due to a reaction between the ceramic coating and the substrate. Some oxidation of the stainless steel would be expected at the higher temperatures. Additional evidence for interfacial reactions includes the colour changes in samples undergoing different thermal treatments. Chromium in a tetrahedral site is often a brilliant red colour. Chromium substituting for zirconium in the tetrahedral sites of the fluorite ZrO_2 crystal structure might produce a reddish hue, hence leaving the red patches in the samples at 850 and 950° C. In contrast $FeCr_2O_4$ is dark brown and $(Fe_{0.6}Cr_{0.4})_2O_3$ is black, which explains the darkening of the samples heat treated at higher temperatures. When the sample heat treated at 850° C underwent the adhesion test, much of the red colour was concentrated near the fractured interface.

Interfacial reactions must be contributing to the strengthening of the interface between the ceramic and substrate. In the coating adhesion data, the sample with no interfacial reaction products (750° C) had as its weakest point the ceramic–metal interface. In the 850° C sample the interface was also weak but in some areas was stronger than the ceramic. The 950° C sample broke entirely within the ceramic, indicating that the interface with the iron chromate interfacial layer was stronger than the ceramic material. Because the last sample (1050° C) exceeded the bonding strength of the epoxy, no useful information about the relative strength of coating compared to interface can be drawn from this test, but the interfacial adhesion must have exceeded 14.5 MPa. This last sample also had the greatest amount of the iron chromate interfacial reaction products, indicating that these phases act as a good "glue" to bond the metal and the ceramic coating together. The lack of corrosive activity also indicates that the coatings heat treated at 1050° C were fairly dense and protective.

TABLE I Adhesion and fracture results

Sample	Fracture stress (MPa)	Mode of failure
750° C	3.2	At ceramic–metal interface
850° C	3.4	Half at ceramic–metal interface Half in ceramic material
950° C	6.7	In ceramic material
1050° C	14.5	At epoxy–ceramic interface

5. Conclusions

1. The sol–gel process utilizing zirconium alkoxide and yttrium acetate is feasible for fabricating yttria-stabilized zirconia coatings.

2. Coatings processed at low temperatures are heavily cracked but these flaws self-heal with crystal-

lization and grain growth during higher temperature heat treatments (1050° C).

3. Interfacial reactions between the stainless steel substrate and the coating form iron chromates. This results in strong interfacial bonding.

4. These coatings are promising for corrosion protection applications under acidic conditions.

Acknowledgements

The authors acknowledge the help of the following colleagues: Joseph Bailey, Yung-Jen Lin and Cheng-Chen Hseuh at the University of Minnesota, and Wally Wallenhorst, Jim Heger and Vernon Pierskalla at the Honeywell Ceramics Center.

References

1. R. J. BRATTON and S. K. LAU, in "Advances in Ceramics," Vol. 3, edited by A. H. Heuer and L. W. Hobbs (American Ceramic Society, Columbus, Ohio, 1981) p. 226.
2. A. G. EVANS, D. B. MARSHALL and N. H. BURLINGAME, *ibid.* p. 202.
3. D. R. UHLMANN, B. J. J. SELINSKI and G. E. WNEK, in "Better Ceramics Through Chemistry," Materials Research Society Symposia Proceedings Vol. 32, edited by C. J. Brinker (Elsevier, New York, 1984) p. 59.
4. M. A. C. G. VAN DE GRAAF and A. J. BURGGRAAF, in "Advances in Ceramics," Vol. 3, edited by A. H. Heuer and L. W. Hobbs (American Ceramic Society, Columbus, Ohio, 1981) p. 744.
5. J. C. DEBSIKDAR, *J. Non-Cryst. Solids* **86** (1986) 231.
6. D. E. BORNSIDE, C. W. MACOSKO and L. E. SCRIVEN, *J. Imaging Technol.* **13** (1987) 122.
7. A. SRIVASTA and M. DONGARE, *Mater. Lett.* **3** (1987) 111.
8. ASTM Designation C633-79. "Standard Test Method for Adhesion or Cohesive Strength of Flame-Sprayed Coatings" (American Society for Testing and Materials, Philadelphia, Pennsylvania, 1979).

Received 12 December 1988
and accepted 23 August 1989